JOURNAL OF CATALYSIS 122, 80–94 (1990)

# The Nature of Catalytic Sites on Lanthanum and Neodymium Oxides for Dehydration/Dehydrogenation of Ethanol

MICHAEL P. ROSYNEK,[1] ROBERT J. KOPROWSKI,[2] AND GREGORY N. DELLISANTE

*Department of Chemistry, Texas A & M University, College Station, Texas 77843*

Received August 24, 1989

The multi-pathway (dehydration/dehydrogenation) conversion of ethanol has been used to investigate the nature and behavior of catalytically active sites on lanthanum and neodymium sesquioxides. Catalytic reaction data, coupled with infrared spectroscopic characterizations of adsorbed species, indicate that at least two different types of catalytically active sites are generated on activated $La_2O_3$ and $Nd_2O_3$ surfaces that are prepared by thermal dehydration of the corresponding trihydroxides. One kind of site (designated Type I) is much less numerous than the other (Type II), but is more strongly basic and has a much higher initial activity for alcohol dehydration, via a probable ethoxide intermediate, at 300–400°C. The parallel alcohol dehydrogenation pathway, on the other hand, occurs only on Type II sites, which also have moderate dehydration activity. The resulting aldehyde product readsorbs exclusively on the more strongly basic Type I sites, where it undergoes a series of secondary condensation reactions that cause a decrease in the overall rate of alcohol dehydration. The comparative behavioral features of the two kinds of sites may be due to differing surface environments, with Type I sites being in structurally more defective and/or more energetic surface locations than are Type II sites. Increases in pretreatment temperature of the oxides cause thermally induced transformations of Type I sites into Type II sites by a surface annealing or restructuring process, with corresponding modifications in the observed catalytic behaviors for the two alcohol conversion pathways. 

## INTRODUCTION

The complexity of the catalytic and surface properties of basic metal oxides is well established (*1–4*). On many of these materials, the presence of several different and distinguishable kinds of adsorption and catalytic sites has been confirmed by selective adsorption processes and the kinetic behaviors of multi-pathway catalytic reactions. Previous studies in our laboratory have provided selected information about the nature, behavior, and mode of generation of catalytically active sites on lanthanum sesquioxide (*1, 2*). We have demonstrated, for example, the profound influence of variations in catalyst preparation and pretreatment conditions, particularly thermal history, on the subsequent activity and selectivity of this material for double-bond isomerization of *n*-butenes. Our most recent investigations have involved the utilization of other, more complex, diagnostic probe reactions, notably the multi-pathway conversion of alcohols, as well as spectroscopic characterization techniques, with the aim of further refining our understanding of the nature of catalytic sites on this oxide. An additional goal has been to extend these studies to include certain other lanthanide sesquioxides, in an attempt to develop a generalized description of catalytic behaviors for this series of basic metal oxides.

The multi-pathway (dehydration/dehydrogenation) conversion of alcohols has frequently been employed as a diagnostic or model reaction for studying the catalytic properties of metal oxides, and several authors have suggested correlations between

[1] To whom all correspondence should be addressed.

[2] Current address: Celanese Chemical Co., Allentown, PA.



0021-9517/90 $3.00

the observed activity/selectivity behaviors of oxides and certain of their chemical/physical properties (*3*). In making such correlations, particular emphasis has been placed upon the importance of acid–base properties of oxides as a key factor influencing catalytic activity (*4*), selectivity (*4, 5*), reaction mechanism (*6*), and mode of water and/or hydrogen elimination (*6–8*). "Acid" catalysts, such as titanium oxide (*9*), alumina (*10*), and silica-alumina (*11*), are traditionally regarded as primarily dehydration catalysts, while "basic" oxides, including zinc oxide (*12, 13*) and the alkaline earth oxides (*14*), are viewed as primarily dehydrogenation catalysts (*11*). Thomke (*15–18*) and others (*5*), however, while recognizing the possible significance of acid–base properties in determining catalytic behavior, have emphasized the concept of elimination mechanism as a more useful criterion for categorizing alcohol conversion over metal oxides. Tamaru and co-workers, for example, have employed a dynamic infrared spectroscopic technique to establish that, at reaction temperatures, an enolate-type species is the principal reaction intermediate during dehydrogenation of 2-propanol over zinc oxide (*12, 13*) and possibly over magnesium oxide as well (*19*).

The difficulties inherent in making such broad generalizations about catalytic behavior, however, are exemplified when an attempt is made to include the lanthanide oxides in such acid–base categorizations. Although the rare earth oxides, particularly the lighter members of the series, are essentially "basic," Tolstopyatova and co-workers, among others, have reported that *both* dehydration and dehydrogenation of ethanol occur, in an approximately 2 : 1 ratio, over the sesquioxides in this series (*20, 21*). The latter studies, however, and most others that have addressed alcohol conversion over rare earth oxides, were performed using samples that had been prepared by thermal decomposition in air of appropriate hydroxides or oxalates precipitated from aqueous solutions of soluble lanthanide salts. This preparation method, although achieving increased catalyst surface areas, does not permit investigation of, for example, the known marked influence of pretreatment evacuation temperature on the two reaction pathways. Additionally, calcination and subsequent handling in air causes the surfaces of these basic oxides to become partially or wholely covered by carbonate entities that result from contact with atmospheric carbon dioxide and that can markedly influence catalytic behavior (*20–22*). The presence of these carbonate species and their effect on catalytic activity for several reactions, including olefin isomerization and alcohol dehydration, have been demonstrated for a variety of metal oxides (*1, 10, 23*). Furthermore, recent studies by Thomke (*18*) indicate that, in contrast to the results of Tolstopyatova (*20, 21*), primary alcohols undergo dehydration but not dehydrogenation over lanthanum and samarium sesquioxides. This contradiction underscores the importance of systematically determing the influences of catalyst preparation method, pretreatment conditions, and surface purity on the observed catalytic behaviors of these oxides.

The present study was undertaken to determine the effects of catalyst pretreatment conditions and of selected adsorbed probe molecules on the activity and selectivity of lanthanum and neodymium sesquioxides for the dehydration/dehydrogenation of ethanol. The intent of the investigation was to obtain more detailed information about the nature and behavior of catalytically active sites on these oxides than has previously been available.

## EXPERIMENTAL METHODS

*Materials.* Lanthanum and neodymium sesquioxides (>99.9% purity) were obtained from Ventron Corp., and these low-surface-area (<1 $m^2/g$) materials were individually convertd into the trihydroxide precursors used in this study by treatment with an excess of triply distilled, deionized water for 16 hr at 100°C. The trihydroxide

products were each filtered, dried in air overnight at 110°C, crushed, and separated into appropriate mesh sizes. Essentially complete (>99%) conversions of both sesquioxides into the corresponding trihydroxides using this procedure were verified by thermally dehydrating samples of the two products and observing mass losses within 0.05% of the expected values (viz., 14.22% for $La(OH)_3 \rightarrow La_2O_3$ and 13.83% for $Nd(OH)_3 \rightarrow Nd_2O_3$).

Preparation of catalytically active forms of lanthanum and neodymium sesquioxides from the trihydroxide precursors was accomplished using methods described previously (*1, 2, 24*). Pretreatment of both catalysts prior to each experiment involved overnight evacuation at 900°C to remove surface carbonate entities and residual reaction species, followed by exposure to 100 Torr of circulating oxygen for 1 hr (with continuous removal of combustion products by an in-line trap maintained at −196°C) and subsequent evacuation for 1 hr at the same temperature. The samples were then quantitatively rehydrated *in situ* to the corresponding trihydroxides by exposure to an excess of gaseous, $CO_2$-free water for either 4 hr at 25°C (in the case of $La_2O_3$) or 16 hr at 100°C (in the case of $Nd_2O_3$), evacuated at the desired pretreatment temperature in the range 400–1000°C for either 16 hr ($La_2O_3$) or 10 hr ($Nd_2O_3$) to a residual pressure of less than $10^{-5}$ Torr, and then rapidly cooled under vacuum to reaction temperature. BET-$N_2$ surface areas of $La_2O_3$ and $Nd_2O_3$ samples prepared by this pretreatment sequence varied inversely with final evacuation temperature and are summarized in Table 1. Catalyst samples (50 mg dehydrated weight) of 20/30 mesh granules were used for both catalysts in all experiments performed at a reaction temperature of 350°C. In experiments involving reaction temperatures of 300 and 400°C, catalyst sample weights were appropriately adjusted to give approximately the same overall rate of conversion as that observed at 350°C.

TABLE 1

Effect of Pretreatment Evacuation Temperature on Surface Areas of $La_2O_3$ and $Nd_2O_3$

| Pretreatment temperature (°C)[a] | Surface area ($m^2/g$) | |
|---|---|---|
| | $La_2O_3$ | $Nd_2O_3$ |
| 300 | 14.5 | — |
| 400 | 14.6 | 17.1 |
| 500 | 13.6 | 14.9 |
| 600 | 12.1 | 14.0 |
| 700 | 10.4 | 13.1 |
| 800 | 7.9 | 11.3 |
| 900 | 4.5 | 9.1 |
| 1000 | — | 5.4 |

[a] Evacuation times, following rehydration, were 16 hr for $La_2O_3$ and 10 hr for $Nd_2O_3$.

Absolute ethanol (>99.9% purity) was obtained from IMC Chemical Group, Inc., and was further purified by repeated vacuum distillations from 25 to −78°C, with final evacuation at −196°C to a residual pressure of $<10^{-4}$ Torr. Helium (99.999%), used as a diluent for the catalytic reaction experiments, and oxygen (99.9%), used during the pretreatment procedure, were Airco high-purity grades, and were further purified before use by passage through a trap at −196°C. Carbon dioxide was Linde instrument-grade (99.99%) and was passed through a trap at −78°C before use. Gaseous water, used for catalyst rehydration during the pretreatment procedure, was taken from the vapor phase over a degassed, saturated solution of $Ba(OH)_2$ stored in a vacuum-tight vessel, which assured $CO_2$ removal via $BaCO_3$ precipitation.

*Apparatus.* All catalytic reaction experiments were performed using a closed-loop, recirculation-type batch reactor (555 $cm^3$ total volume) of a design described previously (*1, 2*). The all-glass reaction system was connected via greased stopcocks to a conventional, mercury-free high-vacuum gas handling system. Initial reactant pressures were measured to ±0.1 Torr using a

low-volume pressure transducer equipped with a digital display. Except where otherwise noted, standard conditions employed for all experiments involved initial ethanol reactant and helium diluent pressures of 50 Torr each and a reaction temperature of 350°C.

Reactant/product mixtures were periodically analyzed by expanding 0.1 vol% samples into the previously evacuated loop of a gas sampling valve on a gas chromatograph. The ethanol reactant and all products, except for $H_2$, were separated using a $\frac{1}{8}$ in. × 10 ft stainless-steel column containing 80/100 mesh Porapak P maintained at 100°C. Hydrogen was separated from the remainder of the reaction mixture in separate samples injected onto a $\frac{1}{8}$ in. × 6 ft column containing 80/100 mesh Linde 5A molecular sieve, also maintained at 100°C. Effluent from the latter column was passed through a $\frac{1}{4}$ in. × 1 ft column containing CuO at 400°C, in order to quantitatively convert eluted $H_2$ into $H_2O$ prior to detection and thereby increase the accuracy of $H_2$ analyses. Quantitative analyses of all reaction mixtures were based on peak areas reported by a recording digital integrator and resulting from the output of a thermal conductivity detector, following calibrated corrections for differing thermal responses of the various components.

Infrared spectra were obtained using a Perkin–Elmer Model 399 spectrophotometer that was interfaced to a microcomputer-based data acquisition and processing system. The latter was used to apply ensemble averaging techniques for signal enhancement and noise reduction that were necessary in order to quantify the relatively weak absorption bands of adsorbed species on the low-surface-area oxide catalysts. The quartz cell employed for these studies was an integral component of a high-vacuum gas handling system and was of standard design, featuring KCl windows and containing a heated region into which the sample could be moved by a windlass arrangement for thermal treatment. Samples were prepared in the form of self-supporting pressed disks having an optical density of 20–30 mg/cm$^2$ and were subjected to the same dehydration/rehydration pretreatment procedure as that used for samples in the catalytic reaction studies. All spectra were recorded in the double-beam transmission mode, using air as a reference, and with the sample at ambient temperature.

X-ray diffraction patterns of powdered $La_2O_3$ and $Nd_2O_3$ samples were obtained using Seifert-Scintag Pad II and General Electric XRD 700 instruments, respectively. Both units were equipped with Cu$K\alpha$ filtered radiation sources and were operated at a voltage of 40 kV and a current of 20 mA. The scan speed was 2°/min in all cases, with a take-off angle of 5°. All oxide samples were prepared for the X-ray diffraction measurements using the same pretreatment method as that employed for the catalytic and infrared samples. The pretreated samples were transferred in a vacuum-sealed vessel to a glovebox, where they were loaded under a dry $N_2$ atmosphere into a sealed and demountable stainless-steel sample holder equipped with a permanently mounted hemispherical Mylar film window that prevented sample contamination by atmospheric water and carbon dioxide during X-ray measurements.

## RESULTS AND DISCUSSION

### *Reaction Products and Selectivity*

In agreement with previously reported results (*20, 21*), we observed that both dehydrogenation (to acetaldehyde) and unimolecular dehydration (to ethylene) of ethanol occurred over the two oxides $La_2O_3$ and $Nd_2O_3$ in the reaction temperature range 300–400°C. (Unimolecular dehydration of alcohols to olefins, rather than bimolecular dehydration to ethers, is commonly observed over metal oxide catalysts at temperatures exceeding ~300°C (*6, 25*).) Figures 1 and 2 present typical product distributions obtained at 350°C over $La_2O_3$ and $Nd_2O_3$, respectively, that had been pre-

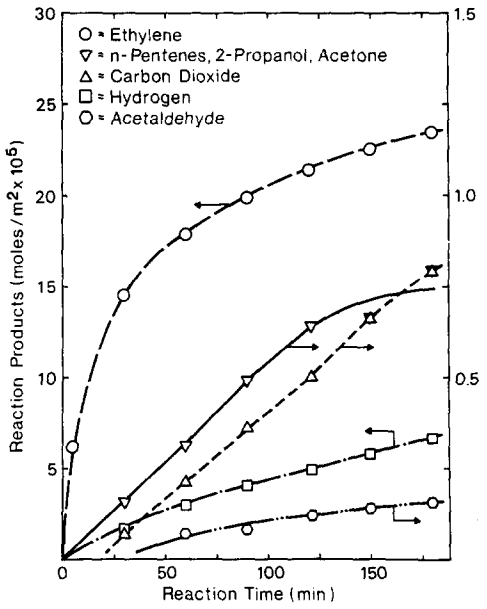


FIG. 1. Reaction product formation during ethanol conversion at 350°C over $La_2O_3$ pretreated at 400°C.

treated at 400°C. Both the activities and reaction selectivities of the two oxides are very similar under these conditions. Indeed, the overall behaviors of the two materials, with certain minor exceptions, closely resembled each other at all reaction and pretreatment temperatures studied, and, unless otherwise noted, all subsequent discussion and interpretation of experimental results applies equally to both oxides.

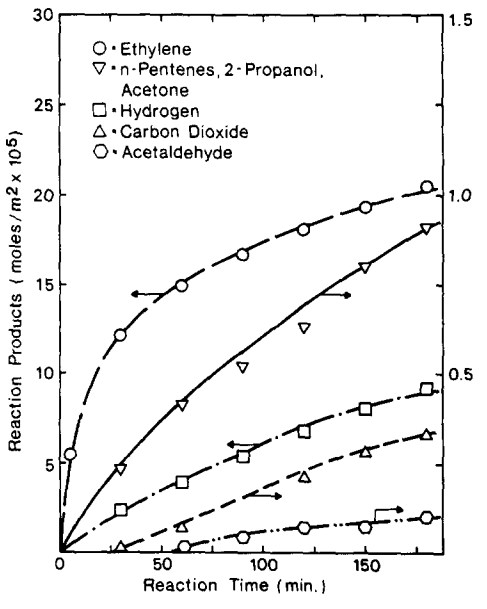


FIG. 2. Reaction product formation during ethanol conversion at 350°C over $Nd_2O_3$ pretreated at 400°C.

The results shown in Figures 1 and 2 demonstrate that, although the dehydration pathway is uncomplicated by the occurrence of secondary reactions, including hydrogenation of the ethylene product by hydrogen formed during the dehydrogenation reaction, the latter pathway is more complex and involves secondary reactions of the acetaldehyde primary product that ultimately produce carbon dioxide, acetone, 2-propanol, and *n*-pentenes. It should be noted that, although simple dehydrogenation of ethanol would generate equimolar amounts of hydrogen and acetaldehyde, the molar amount of gaseous hydrogen product observed over both catalysts greatly exceeds that of the aldehyde throughout the range of reactant conversion shown. Moreover, the discrepancy is only partially accounted for by the observed amounts of secondary products, and the remaining mass imbalance is due to the presence of considerable adsorbed acetaldehyde on the catalyst surfaces. At a reaction temperature of 300°C (Fig. 3), where gaseous acetaldehyde product is absent entirely, the mass imbalance is even greater than at 350°C, while at 400°C (Fig. 4), it is almost negligible, the discrepancy between amounts of hydrogen and acetaldehyde products being almost entirely accounted for by the secondary reaction products.

This description of the prevailing surface processes is supported by the experimental results depicted in Fig. 5, for which acetaldehyde, rather than ethanol, was employed as the reactant at 350°C over a $La_2O_3$ sample pretreated at 400°C. The aldehyde produces hydrogen as its principal reaction product, and the mass loss due to acetaldehyde adsorption (after accounting for total amounts of secondary products) is very nearly twice the amount of gaseous molecu-

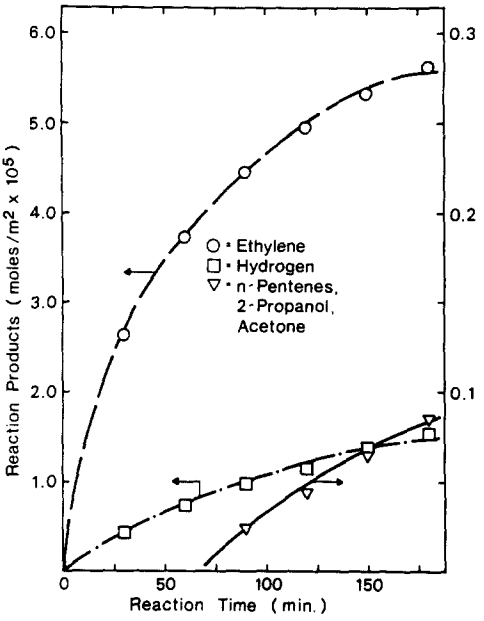


FIG. 3. Reaction product formation during ethanol conversion at 300°C over $La_2O_3$ pretreated at 400°C.

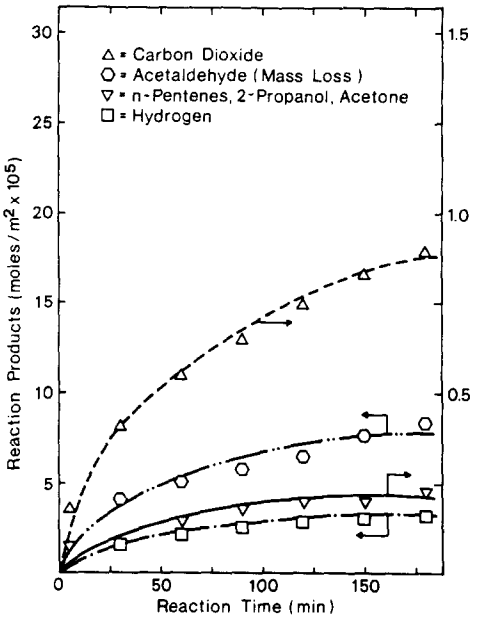


FIG. 5. Reaction product formation and reactant adsorption during acetaldehyde conversion at 350°C over $La_2O_3$ pretreated at 400°C.

lar hydrogen at all conversions shown. Furthermore, the relative amounts of carbon dioxide, acetone, and *n*-pentenes are similar to those observed during ethanol conversion over the same catalyst at this temperature (Fig. 1). These results, together with those of infrared spectroscopic measurements that will be subsequently described, indicate that acetaldehyde dissociatively adsorbs onto the catalyst surface during reaction to form acetate-like species via loss of carbonyl hydrogen atoms. The latter combine to appear as molecular $H_2$, the molar amount of which is thus one-half that of the adsorbed aldehyde. The surface entities derived from adsorbed acetaldehyde then slowly undergo a series of condensation-type reactions with gas-phase ethanol and/or acetaldehyde to form the observed secondary products. These processes probably involve aldol- or Cannizzaro-type condensations, which are known to occur readily on basic catalysts (*26*).

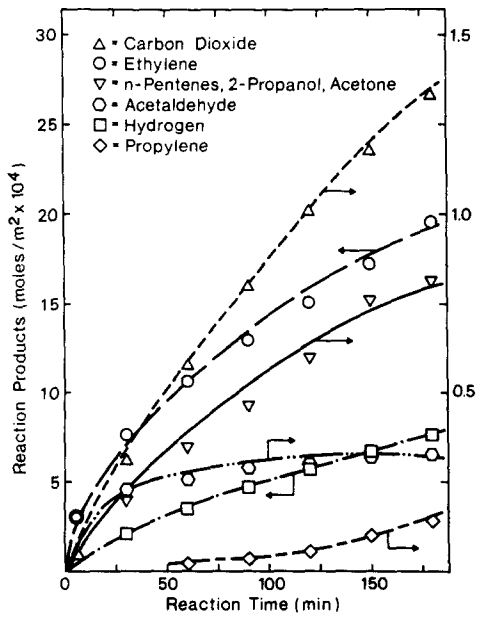


FIG. 4. Reaction product formation during ethanol conversion at 400°C over $La_2O_3$ pretreated at 400°C.

### *Nature and Behavior of the Active Sites*

Information about the nature and behavior of the active sites that are utilized by the two reaction pathways was obtained by investigating the influence of catalyst pre-

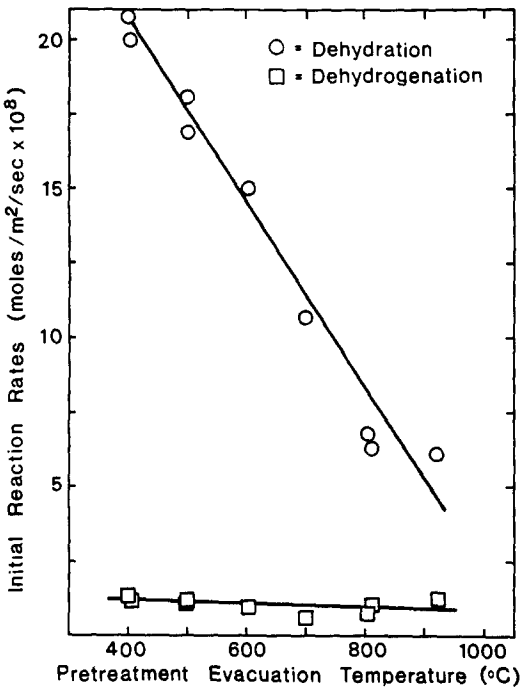


FIG. 6. Effect of catalyst pretreatment temperature on initial rates of ethanol dehydration and dehydrogenation at 350°C over $La_2O_3$.

treatment temperature on the observed dehydration and dehydrogenation rates and by exploring the effect of certain probe molecules on catalytic activity and selectivity. Figure 6 summarizes *initial* reaction rates observed for the two ethanol conversion reactions at 350°C over freshly pretreated $La_2O_3$ samples that had been evacuated at various temperatures in the range 400–900°C. The activities shown for dehydration are based on the initial rates of gaseous ethylene formation. Those indicated for dehydrogenation represent two-thirds of the initial rate of appearance of gaseous hydrogen, since, as noted previously, virtually all of the initially generated acetaldehyde at this temperature quickly readsorbs via loss of carbonyl hydrogen atoms which subsequently combine to produce molecular hydrogen. (Thus, the net result of ethanol dehydrogenation plus acetaldehyde readsorption is the appearance of 1.5 mole of molecular hydrogen for each mole of originally produced acetaldehyde.) It is evident that the initial rate of alcohol dehydration declines continuously with increasing pretreatment temperature in the range investigated, while the initial activity for dehydrogenation, although only 5–15% that of dehydration, is virtually unaffected by variations in prior evacuation temperature. The corresponding activity/selectivity behavior of $Nd_2O_3$ (Fig. 7) is nearly identical to that exhibited by $La_2O_3$, except that the decrease in initial dehydration activity with increasing pretreatment evacuation temperature is less pronounced.

The virtual lack of sensitivity of the initial dehydrogenation reaction rates to changes in catalyst pretreatment temperature indicates that the surface concentration and/or relative activity of the sites utilized during this pathway are not affected appreciably by variations in thermal treatment. The pronounced declines in initial dehydration rates, on the other hand, suggest that the number and/or activity of the most active sites used by this pathway is

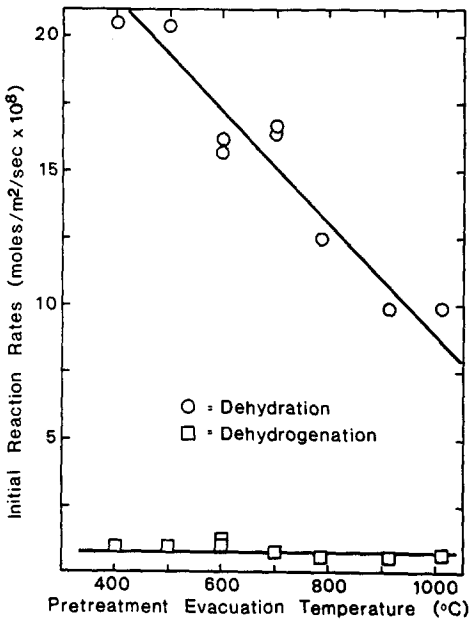


FIG. 7. Effect of catalyst pretreatment temperature on initial rates of ethanol dehydration and dehydrogenation at 350°C over $Nd_2O_3$.

TABLE 2

Effect of Pretreatment Evacuation Temperature on Phase Compositions of $La_2O_3$ and $Nd_2O_3$

| Pretreatment temperature (°C)[a] | $La_2O_3$ | | $Nd_2O_3$ | |
|---|---|---|---|---|
| | % C-Type | % A-Type | % C-Type | % A-Type |
| 300 | 62 | 38 | 100 | 0 |
| 400 | 44 | 56 | 100 | 0 |
| 500 | 31 | 69 | 95 | 5 |
| 600 | 30 | 70 | 89 | 11 |
| 700 | 13 | 87 | 75 | 25 |
| 800 | 0 | 100 | 62 | 38 |
| 900 | 0 | 100 | 30 | 70 |
| 1000 | 0 | 100 | 0 | 100 |

[a] Evacuation times, following rehydration, were 16 hr for $La_2O_3$ and 10 hr for $Nd_2O_3$.

decreased by increasing pretreatment temperature. The observed effect may be caused by one or more of several possible thermally induced phenomena, including crystallographic structure transformations of the two oxides, changes in concentrations of residual surface hydroxyls, or fundamental alterations in the chemical/structural nature of the active sites. Additional experiments were performed in order to ascertain the relative importance of these factors in influencing the observed catalytic behaviors of $La_2O_3$ and $Nd_2O_3$.

At temperatures below 2000°C, the stoichiometric lanthanide sesquioxides can exist in any of three distinct crystalline modifications, viz., the so-called A-type (hexagonal), B-type (monoclinic), and C-type (body-centered-cubic) polymorphs (*27*). Thermally induced transformations (C $\rightarrow$ A and C $\rightarrow$ B) between the three phases of a single oxide are essentially irreversible under anhydrous conditions, and the temperature required to effect such transitions varies inversely with lanthanide cation radius. The lightest (largest cation radius) members of the series ($La_2O_3$ to $Pr_2O_3$) exist primarily in the A-type structure at all temperatures, with the C-form being only metastable. The intermediate oxides ($Nd_2O_3$ to $Dy_2O_3$) assume a stable C-type structure following preparation or treatment at low temperatures (<500°C), but transform to either the A-type ($Nd_2O_3$) or B-type ($Sm_2O_3$ to $Dy_2O_3$) modification at higher temperatures. The heaviest (smallest cation radius) oxides in the series ($Ho_2O_3$ to $Lu_2O_3$) exist only as the C-type polymorph at all temperatures below 2000°C.

Table 2 presents the results of X-ray powder diffraction studies of the effect of pretreatment temperature on phase compositions of $La_2O_3$ and $Nd_2O_3$ samples that had been pretreated using the same dehydration/rehydration/evacuation method as that employed for the catalytic reaction experiments. The relative amounts of the two structures in each case are based on the peak area of the most intense line in the pattern for each polymorph. These are 0.3294 nm (222) for C-$La_2O_3$, 0.3200 nm (222) for C-$Nd_2O_3$, 0.2974 nm (101) for A-$La_2O_3$, and 0.2902 nm (101) for A-$Nd_2O_3$, where the number in parentheses represents the (*hkl*) reflection of the line. All observed *d*-spacings were within 0.001 nm of values reported by previous investigators (*28–31*). The phase compositions shown do not represent thermodynamic equilibrium at the indicated temperatures, because a fixed evacuation time was used in each case, but they do serve to reveal the actual compositions of the catalysts used for the catalytic reaction experiments.

In the case of $La_2O_3$, the metastable C-type phase was not observed in pure form, even following treatment at the lowest temperature (viz., 300°C) at which decomposition of the hydroxide precursor is essentially complete. With increasing temperature of evacuation, the C-type structure gradually transforms into the A-type, with the latter being the only form observed following treatment at $\geq$800°C. With $Nd_2O_3$, the pure C-type structure is obtained at <500°C, and it also transforms into the A-form with increasing temperature, the process becoming complete at 900 to 1000°C. It is apparent, however, that the declines shown in Figs. 6 and 7 for initial alcohol dehydration rates with increasing pretreat-

ment temperature do not directly correlate with the thermally induced structure transformations observed for either of the two oxides. Conversion of C-type $La_2O_3$ to the A-form, for example, is completed between 700 and 800°C, but the initial rate of alcohol dehydration continues to decrease up to the highest pretreatment temperature investigated, viz., 900°C.

The effect on the two alcohol conversion pathways of variations in the concentration of residual surface hydroxyls was also explored. Figure 8 displays the effect of pretreatment temperature on the integrated absorbance intensity of the infrared band at 3590 $cm^{-1}$ that is due to O–H stretching of surface hydroxyl groups on $La_2O_3$ (*22*). It is clear that detectable surface hydroxyls are completely removed from $La_2O_3$ following evacuation at temperatures above 600°C. Analogous results were obtained for $Nd_2O_3$, with complete hydroxyl removal occurring at slightly higher temperatures than those required for $La_2O_3$. Consequently, no correlation can be made between surface hydroxyl concentration and the observed decline in ethanol dehydration rate with increasing pretreatment temperature.

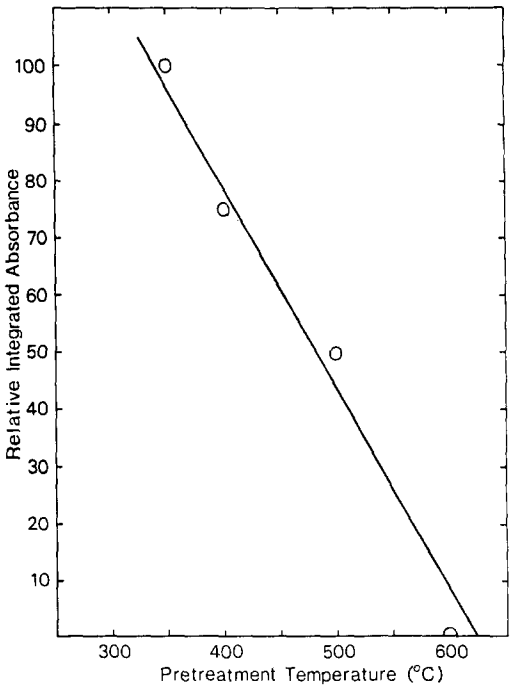


FIG. 8. Effect of pretreatment temperature on relative amount of residual surface hydroxyls on $La_2O_3$.

In order to further investigate the possible influence of residual surface hydroxyls on the catalytic activities of these oxides, a sample of $La_2O_3$ catalyst was pretreated in the usual manner, using a final evacuation temperature of 800°C, cooled under vacuum to 400°C, exposed at the latter temperature to 20 Torr of gaseous water for 1 hr, and then evacuated for 16 hr at the same temperature. The resulting material had a surface hydroxyl concentration virtually identical to that of a normally pretreated sample when the final evacuation temperature was 400°C (as confirmed by a parallel infrared spectroscopy experiment). The catalytic activity of the sample for both alcohol reaction pathways, however, was identical to that of a sample that had been pretreated in the usual manner at 800°C. Hence, although surface hydroxyls may influence the activity and/or selectivity of certain other oxide catalysts for alcohol conversion (*10, 25*), it appears that on $La_2O_3$ and $Nd_2O_3$ such hydroxyls can easily be displaced by reacting ethanol molecules at the reaction temperatures employed for this study and do not affect the rate of either pathway. The observed loss of initial dehydration activity with increasing pretreatment temperature for both oxides is evidently caused by essentially irreversible changes in either the chemical/structural nature or the surface concentration of the active sites. Only complete bulk rehydration to the trihydroxide and subsequent evacuation at a lower temperature can effect recovery of the dehydration activity lost by higher temperature treatment.

The nature of such thermally induced changes in active site properties was investigated using adsorbed carbon dioxide as a probe. In separate experiments, $CO_2$ was exposed in the infrared cell to freshly pre-

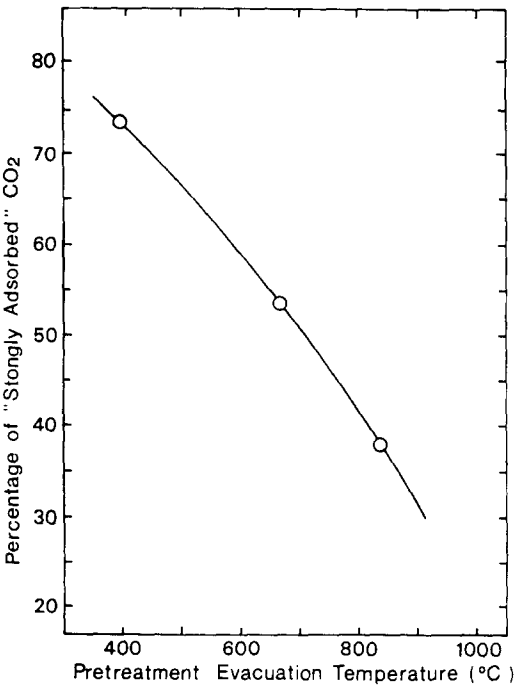


FIG. 9. Effect of pretreatment temperature on capacity of $La_2O_3$ to "strongly" adsorb carbon dioxide.

treated samples of $La_2O_3$ for 1 hr at the ambient infrared beam temperature (viz., 50°C), and then briefly evacuated at this temperature in order to remove weakly adsorbed $CO_2$. The integrated absorbance intensity of the band doublet at 1390 and 1465 $cm^{-1}$, resulting from the doubly degenerate anti-symmetric stretching mode of surface unidentate carbonate species (*23*), was then measured and compared to that observed for the same bands after evacuating the sample for 40 min at 300°C. The ratio of the latter intensity to the former was taken to be a measure of the amount of "strongly adsorbed" $CO_2$ on the sample and is shown as a function of sample pretreatment temperature in Fig. 9. It is evident that the decrease in amount of this strongly adsorbed $CO_2$ with increasing prior pretreatment temperature of the sample closely parallels the corresponding decline in initial alcohol dehydration activity of $La_2O_3$ shown in Fig. 6. This observation suggests that the high initial activity observed for the dehydration pathway on both oxides is primarily due to the most strongly basic surface sites, i.e., those sites that are capable of most strongly retaining adsorbed $CO_2$, and, furthermore, that the surface concentration of these sites is adversely affected by increases in evacuation temperature.

The significance of this correlation was confirmed by experiments in which $CO_2$ was added to the initial ethanol/helium reaction mixture. Figure 10 illustrates the dependence on reaction time of the rates of the two ethanol conversion pathways for three typical runs, with no added $CO_2$, over $Nd_2O_3$ samples pretreated at various temperatures in the range 400 to 1000°C. The results shown were obtained at a reaction temperature of 350°C, but the type of behavior depicted was observed over both oxides throughout the reaction temperature range 300 to 400°C. The initially high dehydration rates decline rapidly with increasing

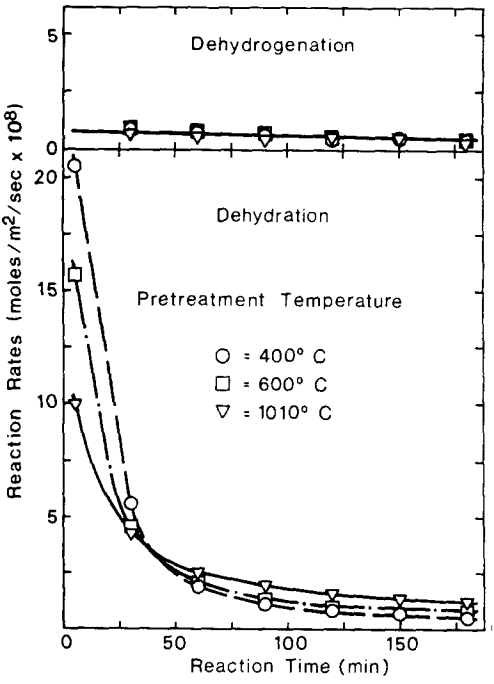


FIG. 10. Dependence of ethanol dehydration and dehydrogenation rates at 350°C on reaction time over $Nd_2O_3$ pretreated at the indicated temperatures.

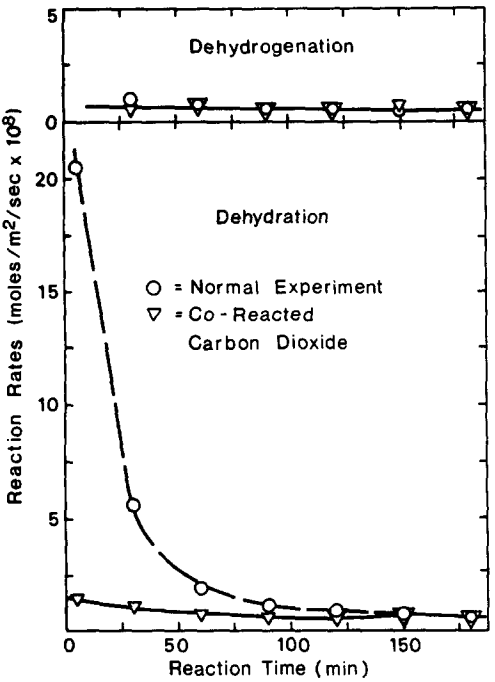


FIG. 11. Effect of coreacted carbon dioxide on ethanol dehydration and dehydrogenation rates at 350°C over $Nd_2O_3$ pretreated at 400°C.

time of exposure to the catalyst and eventually reach much lower, but essentially stable, residual levels. This marked rate decrease is not due to accumulation of product water molecules on the catalyst surface, since addition of 10 Torr of gaseous water to the initial ethanol/helium reaction mixture resulted in the same high initial activity as in the absence of added water. In addition, it should be noted that, although the *initial* activity for dehydration is inversely dependent on catalyst pretreatment temperature, the reverse is true for the lower, residual dehydration rates. In the case of the dehydrogenation pathway, not only is the initial activity virtually independent of pretreatment temperature, as noted previously, but the rate remains essentially constant throughout the course of the reaction.

When an excess (10 Torr) of $CO_2$ was added to the initial reaction mixture at 350°C over a $Nd_2O_3$ sample that had been pretreated at 400°C, the results shown in Fig. 11 were obtained. The *initial* dehydration activity was now nearly the same as the much lower, residual activity that is achieved in a normal experiment after a sufficiently long reaction time. By contrast, the rate of the dehydrogenation pathway (based on molecular hydrogen formation) was unaffected by the presence of the $CO_2$. Very significantly, however, the initial percentage of the acetaldehyde product appearing in the gas phase was more than 10 times greater than that observed in the absence of added $CO_2$, and the secondary products (acetone and *n*-pentenes) resulting from acetaldehyde condensation reactions were almost entirely absent during the early stages of reaction.

These results suggest that certain more strongly basic (Type I) surface sites (i.e., those capable of strongly retaining adsorbed $CO_2$) are responsible for the high initial dehydration activity of the two oxides and are also the sites on which the acetaldehyde product of the dehydrogenation pathway dissociatively readsorbs and undergoes subsequent condensation processes. Accumulation of the adsorbed acetaldehyde entities on these sites causes the observed rapid decline in dehydration activity. Another, more weakly basic type of site (designated Type II), which does not strongly adsorb $CO_2$, is also active for dehydration and is, moreover, the only type of site utilized by the dehydrogenation pathway that produces acetaldehyde. The dehydration activity of these Type II sites is much lower than that of the Type I sites, but, following complete deactivation of the latter by adsorbed acetaldehyde species, they are the only sites available for dehydration and produce the stable, residual dehydration activity that is observed in all cases after sufficiently long reaction times.

It is likely that both of these two types of active sites involve surface $O^{2-}$ ions, but in differing structural environments. Type I sites may, for example, consist of $O^{2-}$ ions that are in structurally more defective and/or more energetic surface locations than are

the Type II sites. With increasing pretreatment temperature, Type I sites may gradually transform into Type II sites by a surface annealing or thermally induced restructuring process, thus causing the observed decline in initial dehydration activity. This postulate is supported by the small but continuous increases in *residual* dehydration activity that occurred for both oxides with increasing pretreatment temperature (Fig. 10). The lack of appreciable change in rate of the dehydrogenation pathway, which occurs only on the Type II sites, with increasing evacuation temperature indicates that the latter are much more numerous than the Type I sites, even at the lowest pretreatment temperature investigated.

*Nature of the Adsorbed Species*

In order to more fully describe the types of surface processes occurring during reaction and to determine the cause of the initial decline in dehydration rate, infrared spectroscopy was employed to investigate the nature and behavior of surface species that result from ethanol and acetaldehyde adsorption onto the two oxide catalysts under typical reaction conditions. The spectra presented have all been corrected for sample background fluctuations by digital subtraction and were obtained using $La_2O_3$; nearly identical behaviors, however, were observed for $Nd_2O_3$. A sample of $La_2O_3$ that had been pretreated at 400°C was exposed to 20 Torr of gaseous ethanol at 350°C for 30 min. Following evacuation for 2 min at 350°C and rapid quenching of the sample to ambient temperature, spectrum a in Fig. 12 was obtained. The band group in the range 1300–1600 $cm^{-1}$ can be ascribed to a surface acetate species, while the relatively sharp doublet with maxima at 1050 and 1100 $cm^{-1}$ is due to an adsorbed ethoxide entity. These species and their respective infrared band assignments are similar to those reported previously for ethanol adsorption on ZnO (*12*), $Al_2O_3$ (*32*), and MgO (*33*).

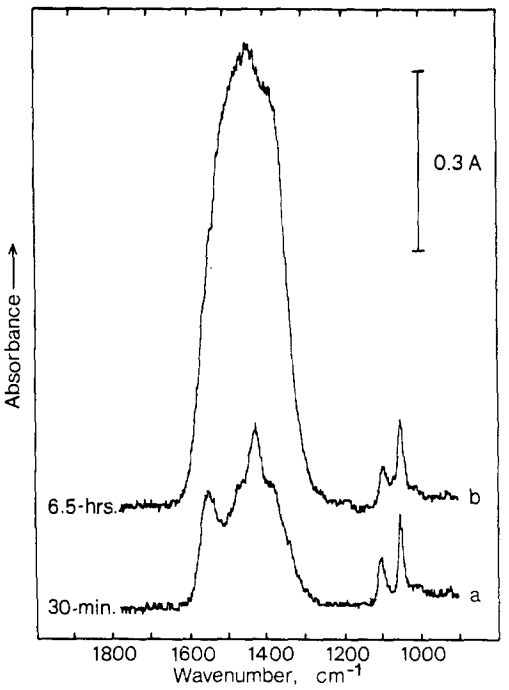


FIG. 12. Infrared spectra resulting from ethanol exposure at 350°C for the indicated times to $La_2O_3$ pretreated at 400°C.

The presence of preadsorbed $CO_2$ (obtained by prior exposure of the sample to $CO_2$ at 350°C, followed by brief evacuation at the same temperature) almost completely suppressed formation of the acetate species, but had virtually no effect on the amount of ethoxide observed. With increasing time of exposure to ethanol, the surface concentration of acetate increased rapidly, as shown in Figs. 12 and 13, but the amount of adsorbed ethoxide remained essentially constant. When these experiments were repeated using a $La_2O_3$ sample that had been pretreated at 800°C (Fig. 14), both the amount and the rate of surface accumulation of the acetate species were substantially lower than those observed for the sample pretreated at 400°C. (Note the differing adsorbance scales in Figs. 12 and 14.) The observed amount of adsorbed ethoxide, on the other hand, was only slightly larger for the latter sample than for the former. For both oxide samples, exposure

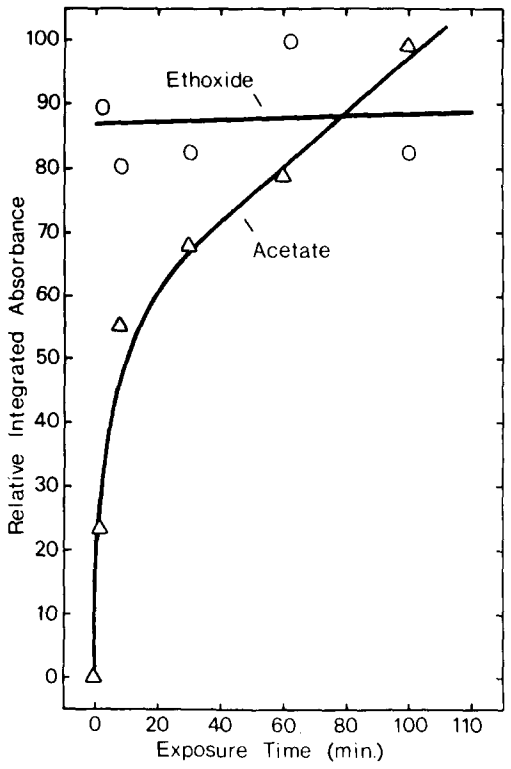


FIG. 13. Effect of ethanol exposure time at 350°C on amounts of surface acetate and ethoxide species formed on $La_2O_3$ pretreated at 400°C.

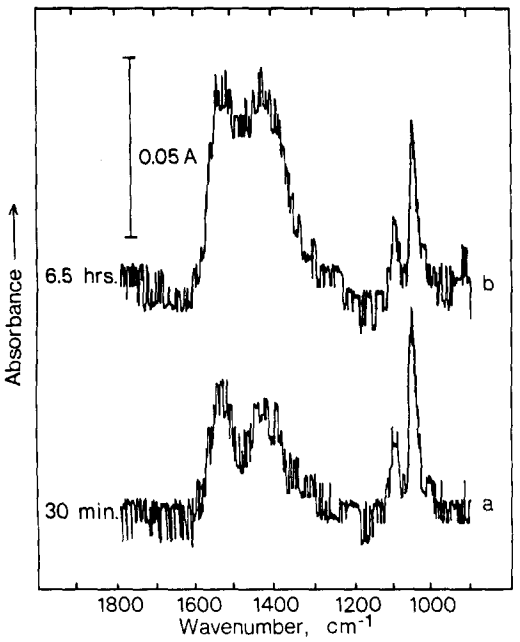


FIG. 14. Infrared spectra resulting from ethanol exposure at 350°C for the indicated times to $La_2O_3$ pretreated at 800°C.

to acetaldehyde produced infrared bands characteristic of the surface acetate species and with intensities approximating those observed following ethanol exposure under the same conditions, but did not generate bands due to the ethoxide entities.

Further insight into the behaviors of these two surface species was obtained by investigating their interaction with each other. Approximately equal amounts of the two species, as shown in spectrum a of Fig. 15, were generated on a $La_2O_3$ sample (pretreated at 400°C) by exposure to ethanol at 350°C for 15 min followed by evacuation for 2 min at the same temperature and then rapid cooling to ambient temperature. When the sample was heated for an additional 15 min at 350°C under dynamic vacuum (thus effecting immediate removal from the cell of desorbed species), the

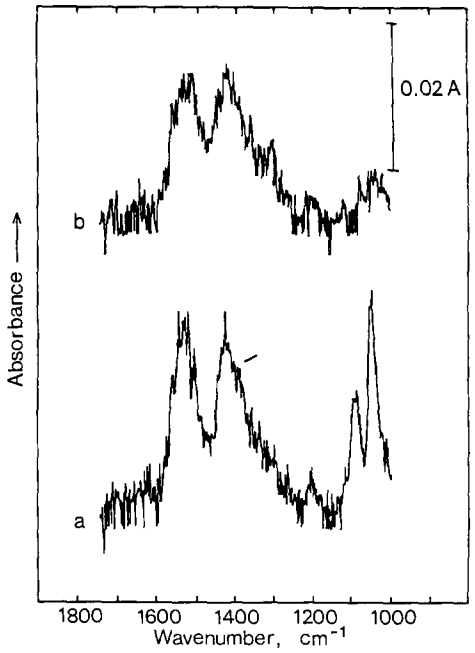


FIG. 15. (a) Infrared spectrum resulting from ethanol exposure at 350°C for 15 min to $La_2O_3$ pretreated at 400°C; (b) following 15 min of evacuation at 350°C.

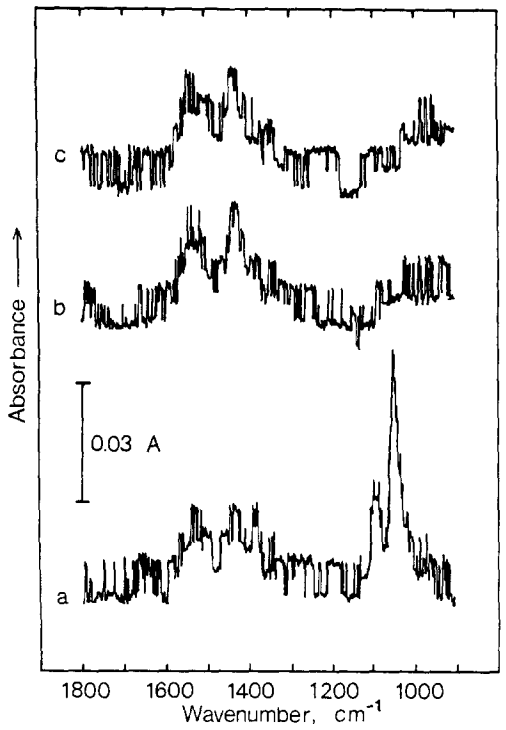


FIG. 16. (a) Infrared spectrum resulting from ethanol exposure at 350°C for 10 min to $La_2O_3$ pretreated at 400°C; (b) following heating for 15 min at 350°C under static vacuum; (c) following heating for an additional 30 min at 350°C under static vacuum.

amount of surface acetate remained virtually unchanged, but most of the original adsorbed ethoxide was removed, as seen in spectrum b of Fig. 15. The experiment was performed a second time, but the additional heating for 15 min at 350°C was made with the cell isolated from the vacuum system, thus allowing readsorption and subsequent surface reaction of the desorbed species. In this case (Fig. 16), the adsorbed ethoxide disappeared completely, and the amount of surface acetate species increased by approximately 35%. In addition, mass spectrometric analysis of the cell contents following the closed-cell heating at 350°C revealed the presence of gaseous ethylene. It is likely, therefore, that decomposition of the adsorbed ethoxide species occurs by both a dehydration pathway that produces ethylene and by a dehydrogenation process that generates acetaldehyde, with the latter undergoing dissociative readsorption to cause the observed increase in amount of surface acetate.

These spectroscopic results are consistent with the postulated dual-site nature of the oxide surfaces and site behaviors that have been discussed in the preceding section and suggest the following view of the surface processes that occur during the alcohol conversion reaction. Initial adsorption of ethanol on the more weakly basic (Type II) active sites of $La_2O_3$ and $Nd_2O_3$ at 350°C occurs dissociatively to produce surface ethoxide species. Ethoxide entities are probably also formed during adsorption on the more strongly basic (Type I) sites, but, due to their apparently high reactivity toward dehydration and consequently short lifetimes on these sites, it is unlikely that they contributed appreciably to the ethoxide bands observed in the infrared spectra. Decomposition of the ethoxide species on Type II sites occurs either by O–C bond breakage (i.e., the dehydration pathway) to ultimately produce ethylene or by hydrogen elimination and desorption of the resultant acetaldehyde (the dehydrogenation pathway). The latter readsorbs dissociatively, via loss of carbonyl hydrogen atoms, on the more highly active Type I sites to generate surface acetate species that participate in secondary condensation processes leading to the formation of acetone and *n*-pentenes. The former can readsorb on Type II sites and undergo hydrogenation to 2-propanol which can, in turn, become dehydrated to propylene on the same sites. The latter product was observed in small amounts during the catalytic reaction studies after sufficiently long reaction times, particularly at a reaction temperature of 400°C (cf. Fig. 4). Accumulation of the strongly held surface acetate on the Type I sites effectively poisons their dehydration activity and causes the observed rapid decline in ethanol dehydration rate with increasing reaction time. The Type II sites are responsible for the residual dehydration activity and for

all of the dehydrogenation activity exhibited by the two oxides.

ACKNOWLEDGMENTS

The authors gratefully acknowledge financial support of this research by the Basic Energy Sciences Division of the U.S. Department of Energy, under Contract DE-AS05-78ER06042, and by the Union/Molycorp Co.

REFERENCES

1. Rosynek, M. P., and Fox, J. S., *J. Catal.* **49,** 285 (1977).
2. Rosynek, M. P., Fox, J. S., and Jensen, J. L., *J. Catal.* **71,** 64 (1981).
3. Krylov, O. V., "Catalysis by Nonmetals." Academic Press, New York, 1970.
4. Tanabe, K., Hattori, H., Sumiyoshi, T., Tamaru, K., and Kondo, T., *J. Catal.* **53,** 1 (1978).
5. Noller, H., and Kladnig, W., *Catal. Rev.* **13,** 149 (1976).
6. Noller, H., Andreu, P., and Hunger, M., *Angew. Chem. Int. Ed. Engl.* **10,** 172 (1971).
7. Siddhan, S., *J. Catal.* **57,** 191 (1979).
8. Lundeen, A., and Hoozer, R., *J. Org. Chem.* **32,** 3386 (1967).
9. Carrizosa, I., and Manuera, G., *J. Catal.* **49,** 189 (1977).
10. Knözinger, H., *in* "Advances in Catalysis," **25,** 184 (1975).
11. DeBoer, J., and Visserer, W., *Catal. Rev.* **5,** 55 (1971).
12. Koga, O., Onishi, T., and Tamaru, K., *J. Chem. Soc. Faraday Trans. 1* **76,** 19 (1980).
13. Akiba, E., Soma, M., Onishi, T., and Tamaru, K., *Z. Physik. Chem. Neue Folge* **119,** 103 (1980).
14. Szabo, Z., Jover, B., and Ohmacht, R., *J. Catal.* **39,** 225 (1975).
15. Thomke, K., *Z. Physik. Chem. Neue Folge* **105,** 87 (1977).
16. Thomke, K., *Z. Physik. Chem. Neue Folge* **106,** 225 (1977).
17. Thomke, K., *Z. Physik. Chem. Neue Folge* **106,** 295 (1977).
18. Thomke, K., *Z. Physik. Chem. Neue Folge* **107,** 99 (1977).
19. Takezawa, N., Hanamaki, C., and Kobayashi, H., *J. Catal.* **38,** 101 (1975).
20. Tolstopyatova, A. A., Balandin, A. A., and Ch' i-ch'uan, Yu., *Zh. Fiz. Khim.* **37,** 2034 (1963).
21. Tolstopyatova, A. A., Ch'i-ch'uan, Yu., and Dulitskaya, K. A., *Izv. Akad. Nauk SSSR Ser. Khim.* **12,** 2095 (1963).
22. Bernal, S., and Trillo, J., *J. Catal.* **66,** 184 (1980).
23. Rosynek, M. P., and Magnuson, D. T., *J. Catal.* **48,** 417 (1977).
24. Rosynek, M. P., and Magnuson, D. T., *J. Catal.* **46,** 402 (1977).
25. Pines, H., and Manassen, J., *in* "Advances in Catalysis" (D. D. Eley, H. Pines, and P. B. Weisz, Eds.), Vol. 16, p. 49. Academic Press, New York, 1966.
26. Komarewsky, V., and Coley, J., *in* "Advances in Catalysis" (W. G. Frankenburg, V. I. Komarewsky, and E. K. Rideal, Eds.), Vol. 8, p. 207. Academic Press, New York, 1956.
27. Eyring, L., *in* "Handbook on the Physics and Chemistry of Rare Earths" (K. A. Gschneider, and L. Eyring, Eds.), Vol. 3, p. 337. North-Holland, Amsterdam, 1979.
28. Felsche, J., *Naturwissenschaften* **56,** 212 (1969).
29. Glushkova, V. B., and Boganov, A. G., *Izv. Akad. Nauk SSSR Ser. Khim.* **7,** 1131 (1965).
30. Swanson, H. E., Fuyat, R. K., and Ugrinic, G. M., *Natl. Bur. Stand. (US)* Circ. No. 539 **3,** 33 (1954).
31. Swanson, H. E., Fuyat, R. K., and Ugrinic, G. M., *Natl. Bur. Stand. (US)* **4,** 26 (1955).
32. Greenler, R. G., *J. Chem. Phys.* **37,** 2094 (1962).
33. Kagel, R. O., and Greenler, R. G., *J. Chem. Phys.* **49,** 1638 (1968).